

EFFECTS OF SOLAR PLASMA AND  
ELECTROMAGNETIC RADIATION  
IN THIN FILMS

National Aeronautics and Space Administration

2

CR-50,531

ARF-A188-5  
(Final Report)

EFFECTS OF SOLAR PLASMA AND ELECTROMAGNETIC  
RADIATION IN THIN FILMS

March 15, 1961 to March 14, 1962

Contract No. NASr-29

Prepared by  
Lawrence C. Scholz

of

ARMOUR RESEARCH FOUNDATION  
of Illinois Institute of Technology  
Technology Center  
Chicago 16, Illinois

for

Office of Research Grants and Contracts  
National Aeronautics and Space Administration  
Code BG  
Washington 25, D. C.

May 1963

ARMOUR RESEARCH FOUNDATION OF ILLINOIS INSTITUTE OF TECHNOLOGY

## TABLE OF CONTENTS

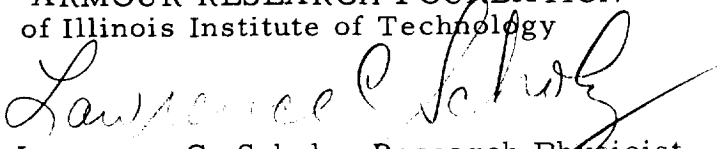
	<u>Page</u>
I. INTRODUCTION-----	1
II. LOW ENERGY SPUTTERING OF THIN FILMS-----	3
Technique of Measurements-----	3
Preparation of the Crystals-----	4
Calculation of the Sputtering Ratio-----	6
III. ELECTRON BOMBARDMENT OF QUARTZ-----	18
Experimental Results-----	20
IV. SPUTTERING BY HIGH ENERGY ARGON IONS-----	26
REFERENCES-----	29
APPENDIX A - REQUIREMENTS OF AN ULTRA-HIGH VACUUM SPUTTERING FACILITY-----	A-1
APPENDIX B - STATIC ULTRA HIGH VACUUM SYSTEM-----	B-1

## FOREWORD

This is the final report on Project A188, and has been prepared for NASA by the Armour Research Foundation of Illinois Institute of Technology under Contract NASr-29, which was administered by Mr. Herbert Talkin of the Office of Research Grants and Contracts at NASA Headquarters. The work was performed in the period 15 March 1961 to 14 March 1962, and reported in a series of four quarterly reports. This final report is a summary of the work presented in those reports. L. Reiffel, Robert Pohl and Lawrence Scholz were the main contributors to the research. We want to thank Sam Webb and George Novotny for their assistance in making the measurements. We would also like to thank Dr. Jaques O'Vadia of Michael Reese Medical Center for allowing us to use the linear accelerator and for his help in setting up the irradiation experiment.

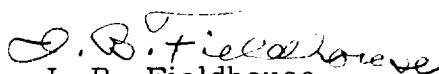
Respectfully submitted,

ARMOUR RESEARCH FOUNDATION  
of Illinois Institute of Technology

  
Lawrence C. Scholz, Research Physicist  
Plasma and Electron Physics Research

APPROVED BY:

  
S. W. Kash, Manager  
Plasma and Electron Physics Research

  
I. B. Fieldhouse,  
Assistant Director of Physics Research

LCS/bw  
5-28-63

ARMOUR RESEARCH FOUNDATION OF ILLINOIS INSTITUTE OF TECHNOLOGY

## ABSTRACT

18414

This is a summary report of work done on sputtering and related phenomena expected for a space vehicle on an interplanetary mission. Preliminary design data for an ultra high vacuum system is given. Sputtering of single and multi-layer films is discussed and data is presented. The coloring and bleaching of quartz in the presence of high energy electrons and intense ultraviolet radiation is discussed and preliminary data is presented.

# EFFECTS OF SOLAR PLASMA AND ELECTROMAGNETIC RADIATION IN THIN FILMS

## I. INTRODUCTION

At the time this work was undertaken there was a general lack of reliable data on sputtering rates for light ions; on threshold values for all ions; and on the density and energy spectrum of the solar protons. This program was therefore directed towards a study of these basic problems. The ultimate aim was a complete understanding of the sputtering process for light ions under condition to be met in interplanetary space. This implies high vacuum conditions and the presence of other forms of radiation, namely solar ultraviolet.

In order to do a definitive experiment with low-energy light-ions, one must have clean surfaces, which implies ultrahigh vacuum conditions. Therefore, a tentative design for an UHV system was made after consultation with equipment manufactures and other workers in the field. As an interim approach, in the absence of a dynamic system, sputtering of thin films in a clean static system was carried out. This experiment was intended to investigate the kinetics of multi-layer sputtering, and to provide the techniques to be used in later studies. Single and multi-layer films, of the noble metals and aluminum, on quartz substates were studied.

Many of the active surfaces of a satellite (i. e. solar cells and other detectors) are protected by glass or quartz windows. These windows or protective layers are susceptible to damage. The mechanisms may include low energy proton sputtering, coloring or other damage from high energy

particles, and other effects attributable to the intense solar ultraviolet radiation. We studied the formation and bleaching of color centers in reasonably pure fused silica. A linear accelerator was used as a source of high energy electrons (30 Mev). Dose rates of  $10^6$  Rad/min, on a 1 mm spot, were obtained. Bleaching history curves were also obtained using a xenon arc lamp.

## II. LOW ENERGY SPUTTERING OF THIN FILMS

The main purpose of this experiment, was to study the effects of film thickness on the sputtering ratio of various metallic films. We had considered fairly heavy films in the range of 250 - 2500 Å. These were generally completely removed during the course of the experiment so that the effects cited below occur at thicknesses much less than this. A useful definition of a thin film for our purposes is one where the impinging particles penetrate an appreciable fraction of its thickness so that energy and momentum transfer is affected by the interface at the boundary of the substrate. We have noted some effects, but additional work would be required to make a quantitative result of this.

### Technique of Measurements

The measurements were made with the change in frequency of quartz crystals technique of McKeown.<sup>(1)</sup> The sputtering was done in the static vacuum system described in our previous report ARF 1188-3. This system was capable of pressures of about  $10^{-8}$  torr after degasing the electrodes by running a discharge. There was initially a severe problem with contamination of the silver films. This was solved with a change in some of the crystal holder parts, and through the introduction of a finely divided silver powder getter. The original aim was to run this system at about  $10^{-5}$  torr and use a very simple technique to generate a small ion current. There was a problem with leakage due to evaporation of tungsten from the electron source and we decided to run the tube as a cold cathode discharge at a rather high pressure of 80 - 100 microns. This technique suffers from certain defects especially with the particular geometry we had chosen. However, we felt



that it was desirable to make these measurements before attempting a major revision. The ions have an excessive energy spread and our control over the total energy was limited.

### Preparation of the Crystals

Commercially<sup>\*</sup> available 10 mc/s AT cut crystals are used. These are matte finished and have silver electrodes of a nonuniform thickness already evaporated unto the quartz. Our films are evaporated unto this silver substrate. No difficulty was experienced in laying down silver, gold, aluminum or germanium films. The crystal frequency is monitored continuously during the evaporation so that the frequency change due to the added mass, or thickness, is known. The thickness of the added layer is determined by placing a glass slide adjacent to the crystal during the evaporation and measuring this film. Attempts to measure the thickness on the crystal directly were unsuccessful because of the matte finish. Optically polished crystals with silver, aluminum or no electrodes are available from the supplier, and would be preferable for future work. The glass slide is masked so as to provide a sharp step in the film. The film thickness is determined with a Bausch and Lomb interferometer microscope objective by measuring the fringe shift. One fringe shift with the 5100 Å line corresponding to  $10^{-5}$  inch or 2540 Angstroms. The estimated accuracy is about 5 percent. With the thickness known one can then determine the mass, assuming the density is that of the normal bulk material. One cannot calculate the mass directly because of the uncertainties in the evaporation process. Past experience in this laboratory indicates that the densities of evaporated films are within 10 percent of the bulk density.

<sup>\*</sup>James Knight Company, Sandwich, Illinois.

The prepared crystals are then put into the discharge tube and the tube is pumped until the low pressure can be maintained. A Vac-Ion pump is used which eliminates pump oil and other contaminants from the system. The glass system has been out-gased by heating with a hot air gun. Spectroscopically pure argon is admitted and the glow discharge established. A shield limits the size of the bombarded spot on the crystal. We had attempted to use tank argon, but had difficulties with impurities even after scrubbing and drying the gas.

These crystals are very stable, and exhibit a total frequency excursion of 10 cycles in the range of temperature from 20 to 100 degrees centigrade,\* with perhaps a two cycle change for a ten degree spread around twenty degrees. No temperature stabilization was used in this work, but it would be required if one attempted to utilize the technique to its fullest. The frequency is monitored with a General Radio model 1130 A counter and its auxillary equipment. This gives a direct record on a paper chart. The current is also monitored during the run. For accurate measurements during long runs some permanent record of current should be made, because there is some difficulty in holding the discharge constant during a long run. The measurements reported here have generally required only relatively short runs. There is a contamination problem in that the argon is depleted and other impurities show up after the discharge runs for awhile. Some measurements had to be made in stages, but this does not seem to effect the final result. The area of the sputtered spot is measured after a run and may be used to determine the number of atoms removed since we know the thickness removed and have assumed a density.

---

\*The details are given in Appendix B.

### Calculation of the Sputtering Ratio

The change in frequency of the quartz crystal as mass is added or deleted can be related to the fundamental oscillating or eigenfrequency of the crystal and the crystal dimensions. For a typical AT cut crystal vibrating in transverse shear, the frequency is essentially set by the time it takes a transverse shear wave to travel through the thickness of the crystal and back, so that<sup>(2)</sup>

$$f = \frac{v_{tr}}{2d} .$$

The thickness of mass added to the crystal is regarded by the crystal as an extra thickness of quartz. If  $A$  is area of the crystal,  $\Delta m$  the added mass, and  $\rho$  the density of quartz ( $2.65 \text{ gm/cm}^3$ ) then

$$\frac{\Delta f}{f} = - \frac{\Delta d}{d} = - \frac{\Delta m}{\rho A d} \quad (\text{II-1})$$

or

$$\frac{\Delta f}{\Delta m} = - \frac{f}{\rho A d} . \quad (\text{II-2})$$

For the 10 Mc crystals used in our experiments, this value is calculated to be

$$\frac{\Delta f}{\Delta m} = 2.28 \times 10^8 \text{ cycles per gram.}$$

This simple picture has to be modified to take into account the area relative to the crystal size over which the mass is added or taken off, because of boundary and more complex mode effects. If the diameter of the spot is 4 mm or more these effects are small. <sup>(2)</sup> In the calculations below we will use the experimentally determined value of  $\Delta f / \Delta m$  for each case.

The sputtering ratio is the ratio of the number of atoms ejected per incident ion. The number of atoms in a gram atomic weight is Avogadro's number,  $N = 6.02 \times 10^{23}$ . So the number of atoms in one gram is  $N/M$ , where  $M$  is the atomic weight. If we let  $k = (\Delta f / \Delta m)_{\text{exptl}}$ , then the actual mass of material sputtered off is  $\Delta f / \Delta k$  grams. Hence the number of atoms sputtered off will be

$$n_{\text{atoms}} = \frac{\Delta f}{k} \frac{N}{M} . \quad (\text{II-3})$$

If we assume that the incident ions are singly ionized and that there are no secondary electrons, then the number of incident ions is simply the incident charge divided by the charge per ion, or

$$n_{\text{ions}} = \frac{\Delta Q}{e} , \quad (\text{II-4})$$

where  $\Delta Q$  is the charge incident during the frequency change  $\Delta f$ , and  $e$  is the charge on an electron,  $1.6 \times 10^{-19}$  coulomb. Hence the sputtering ratio, for the above assumptions, is

$$S = \frac{eN}{M} \frac{\Delta f / \Delta Q}{\Delta f / \Delta m} \quad (\text{II-5})$$

Some error will arise in practice since the area of the incident beam is not always the same as the evaporated spot, and the ion beam does not exactly overlap the evaporated region.

The experimental data for a series of runs using dots of silver, gold, aluminum, and germanium evaporated onto electroplated silver is given in Figures II-1 through II-5. The results of these experiments are summarized in Table I. In an additional experiment listed in the table a single crystal of high purity germanium was sputtered and its change in photoconductivity with bombardment was measured.

The apparent sputtering ratio, as reflected in the change in frequency per unit incident charge, shows an abrupt change during the run. This is seen in the figures, for example in run #5, Figure 2, the transition from aluminum to silver is clearly evident by a slope change by a factor of almost four. Yet the calculated sputtering ratio of the aluminum is higher than that of the silver, because the atomic weight enters in the denominator of the sputtering ratio equation. The sputtering ratio of silver would be expected to be about six times higher than that of aluminum,<sup>(3)</sup> for incident argon ions of 100 volt energy. One possibility that might explain this discrepancy is the spread in the ion energy and the lack of precise control over the actual ion energy. Because of the geometry and pressure used in the discharge tube the ion energy was not as well controlled as desired. The sputtering yield in this low energy region is very dependent on surface conditions. This is a primary argument for the use of ultra-high vacuum techniques.

The small penetration of the lattice by these low energy ions can be inferred from the photoresponse of a germanium single crystal as shown in

TABLE II-1

## SUMMARY OF THIN FILM SPUTTERING EXPERIMENTS

Run No.	Film Mat.	Predicted Thickness Angstroms	Measured Thickness Angstroms	$\Delta f/\Delta m$ cycles/gm $\times 10^{-8}$	Film $f/Q$ cycles/Coul $\times 10^{-4}$	Substrate $f/Q$ cycles/Coul $\times 10^{-4}$	Film S	Substrate S	Remarks
2	Ag	—	1360	5.17	144	213	2.43	3.6	Small break
3	Au	1000	680	6.09	160	181	1.37	2.8	Small break
5	Al	2-3000	5320* or 2800	5.8 or 11.8	.143	0.55	0.0093 0.0045	0.0089 0.0041	Good break
6	Al	0.14 of #5	230	21.5	13.8	192	0.24	0.835	Good break
10	Ge	3800	2650	4.45	5.7	91	0.178	1.92	Good break

\*This uncertainty is due to the uncertainty in the fringe shifts. The shift being either 2.1 or 1.1

Figure II-7. The photoresponse drops to a very small value during sputtering and then returns to normal with a time constant of the order of four minutes. This appears to be the time constant for filling surface recombination and trapping levels with the energy gap of the germanium. Bulk damage would not be as likely to anneal so rapidly at room temperature.

The interpretation of the transition region in Runs No. 6 and No. 10, Figure II-4 and Figure II-5 respectively, probably does not involve the question of ion range, and relative absorption in the two different elements, but rather just the nature of the interface of the two, the uniformity of the ion beam current density across the crater, and perhaps crater edge effects. For instance if the evaporated layer is slightly porous or does not cover uniformly, then the beam will penetrate into the substrate and sputter it. Thus the slope of the measured frequency versus charge curve will increase from the bulk evaporated film value to that of the substrate. The extent of the transition region is then a measure of the porosity, or say the hill-and-dale structure of the interface. A non-uniform ion current density will cause erosion of the evaporated film at the crater center first and finally at the periphery. This will cause a gradual change in the sputtering ratio rather than the abrupt change expected.

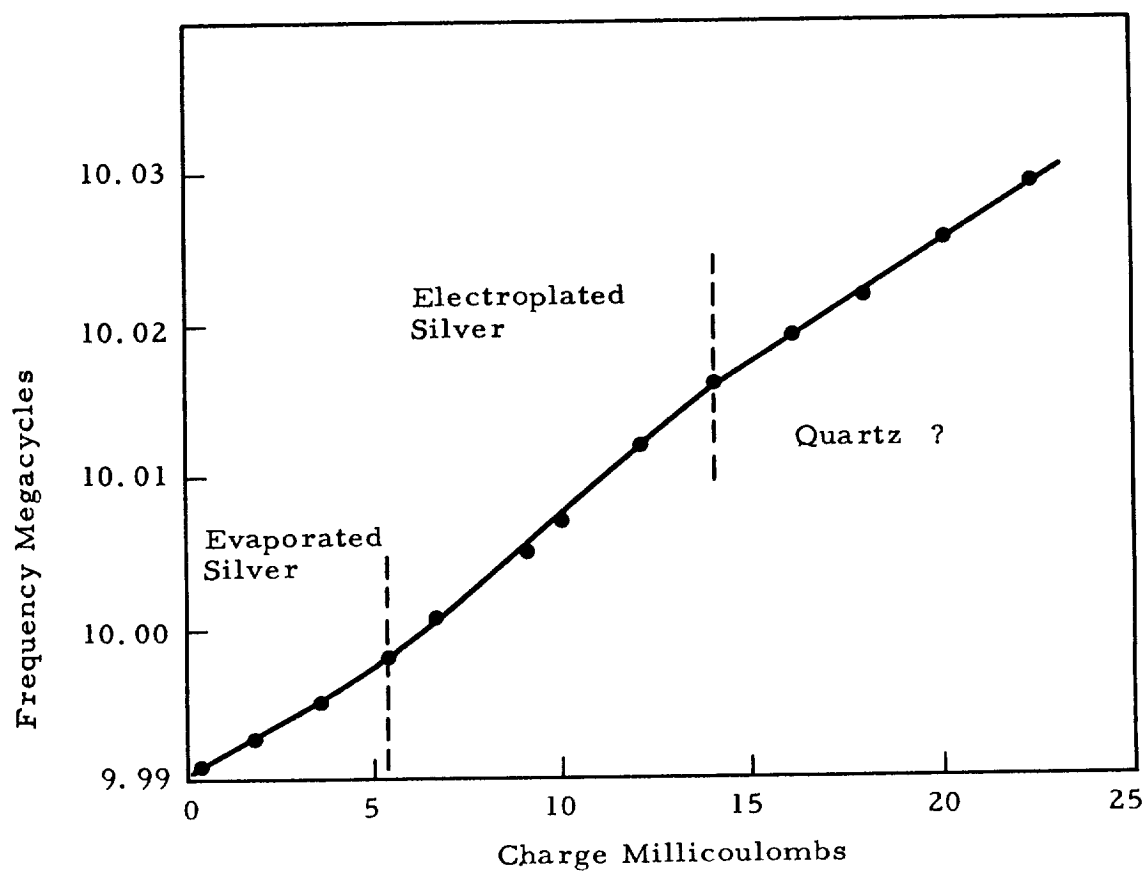


Figure II-1 Sputtering Run No. 2 Silver on Silver Electrodes

17



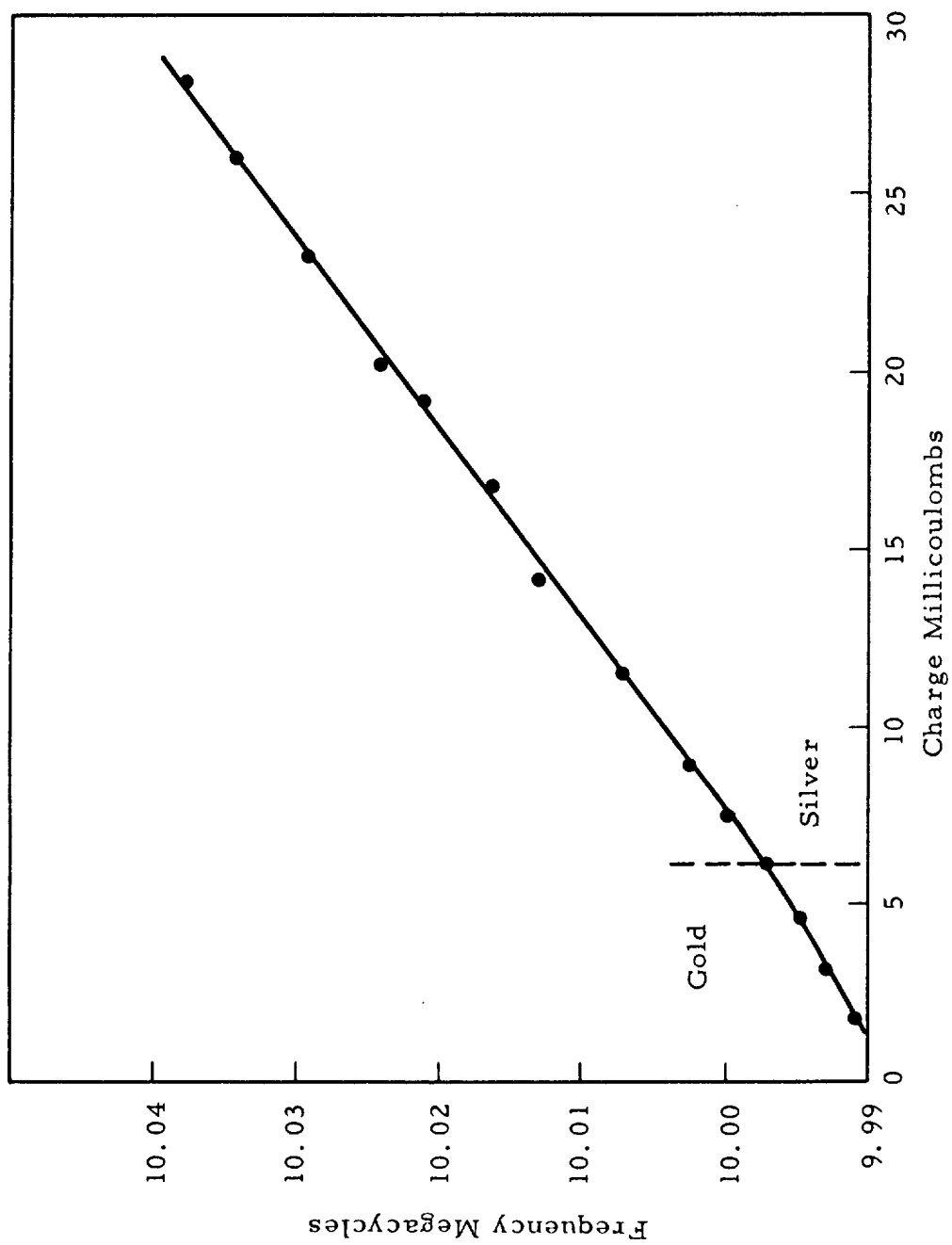


Figure II-2 Sputtering Run No. 3, Gold on Silver, Argon Ions Incident

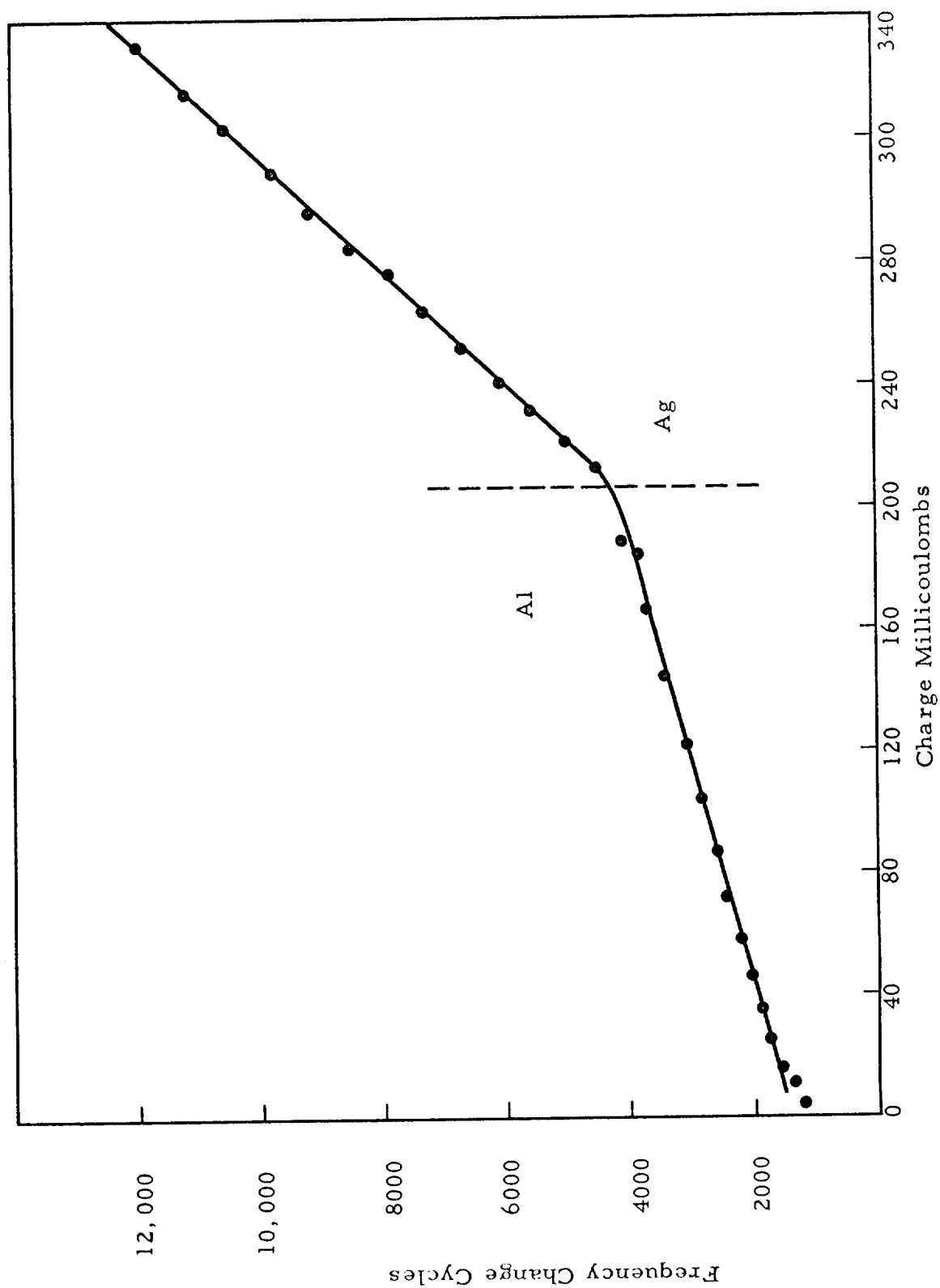


Figure II-3 Sputtering Run No. 5, Aluminum on Silver, Argon Ions Incident

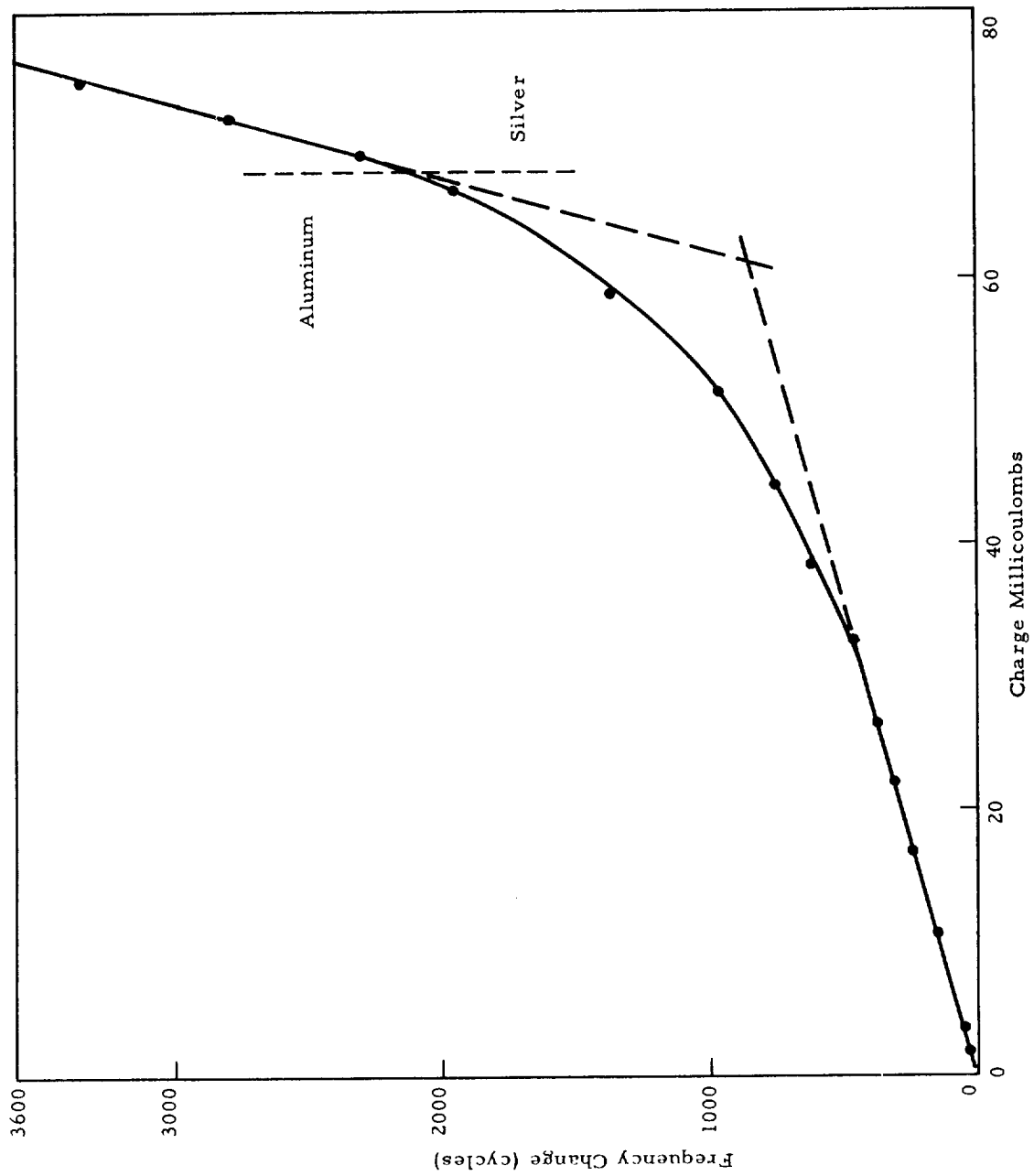


Figure II-4 Sputtering Run No. 6, Aluminum on Silver, Argon Ions Incident

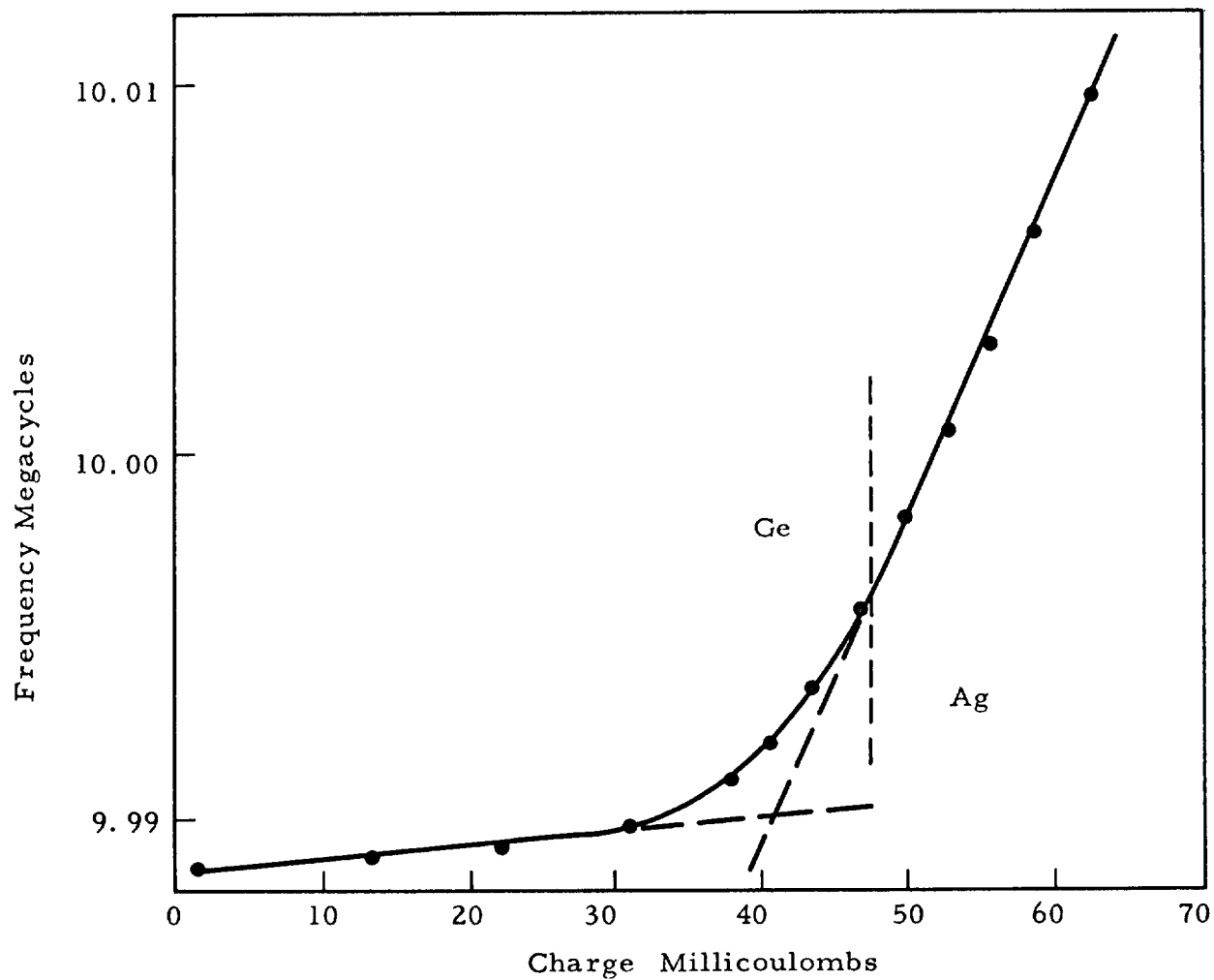


Figure II-5 Sputtering Run No. 10, Germanium on Silver,  
Argon Ions Incident

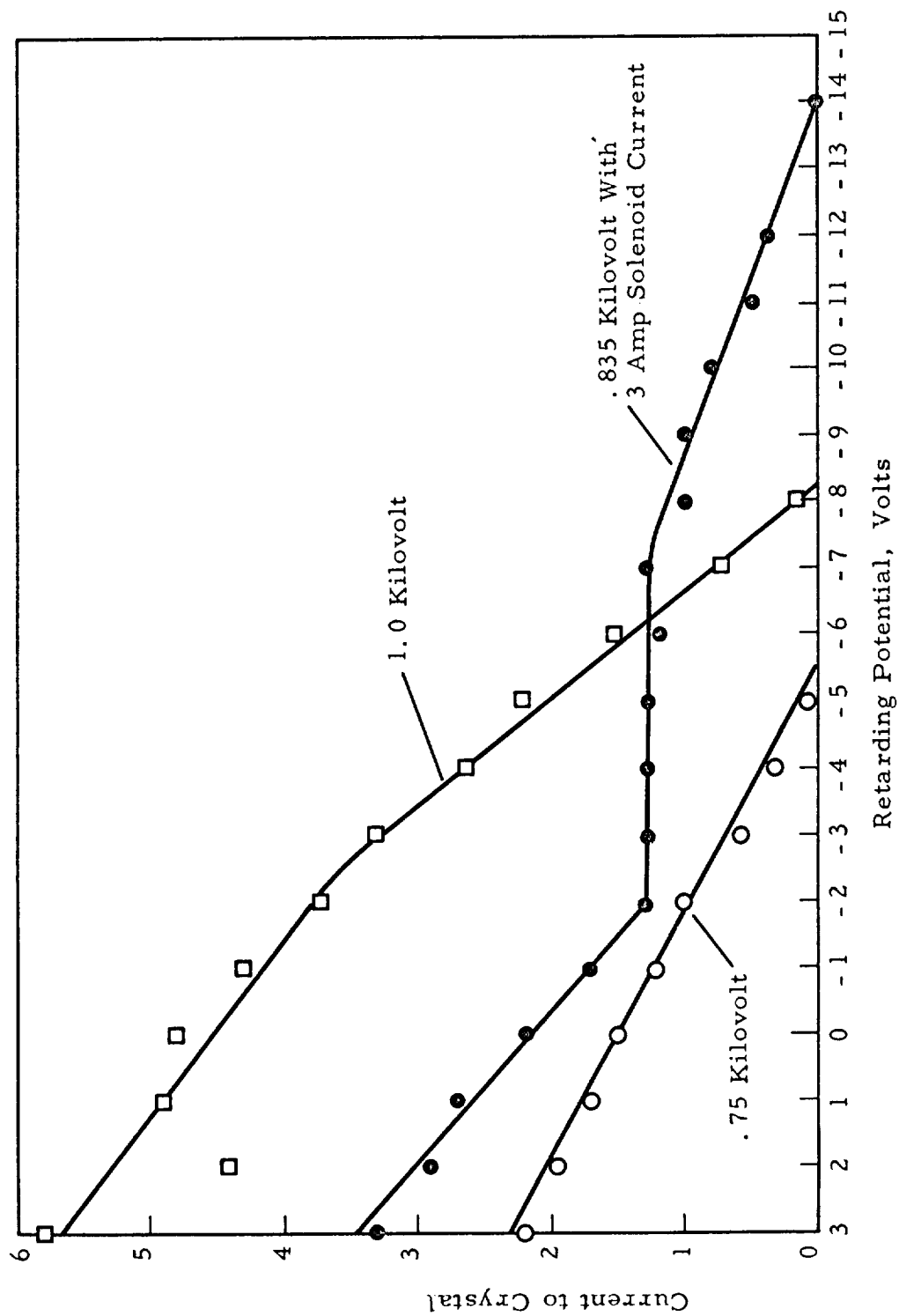


Figure II-6 Ion Energy Determination

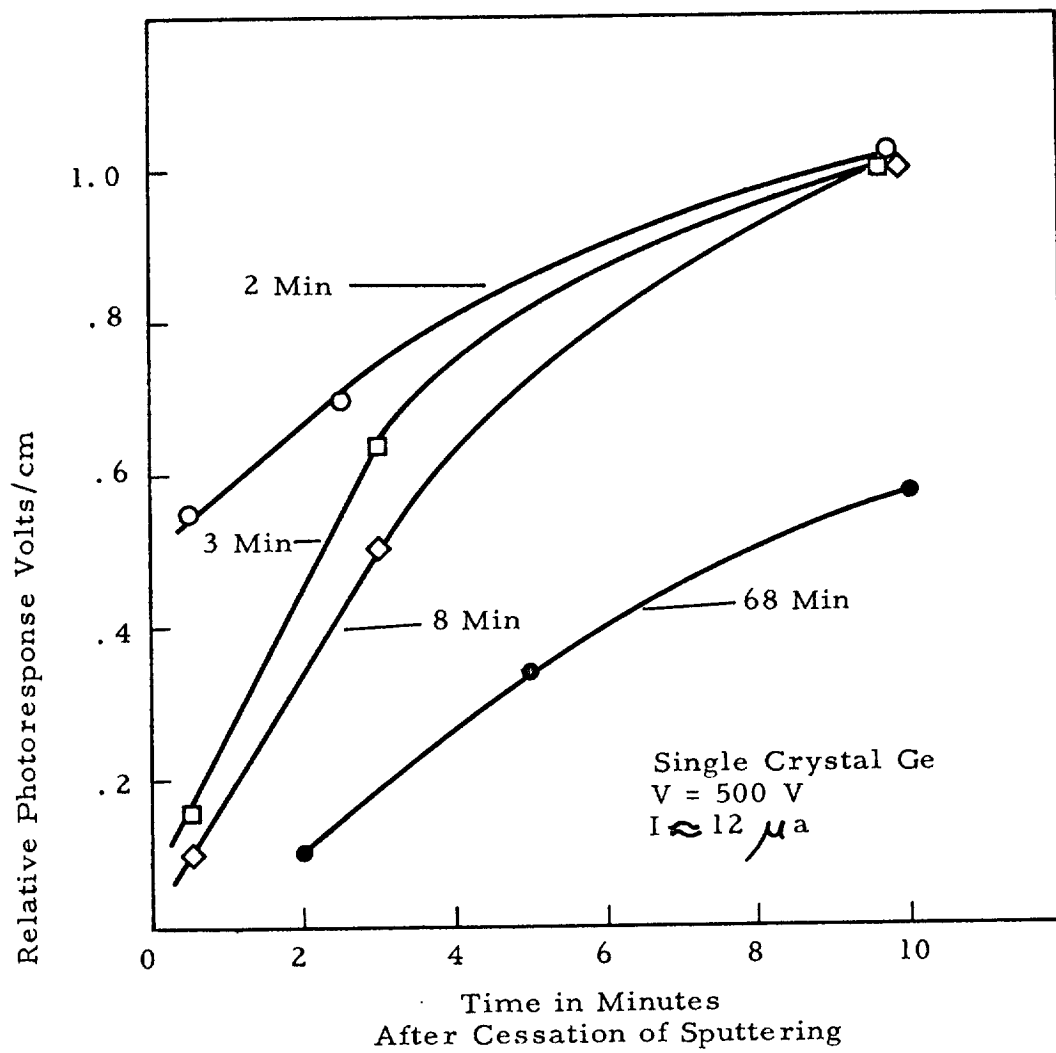


Figure II-7 Photoresponse of Sputtered Germanium

### III. ELECTRON BOMBARDMENT OF QUARTZ

Although this program was to be mainly concerned with sputtering and other damage in the solar plasma there is an allied problem of great interest which concerns the radiation damage due to high energy particles. This problem could assume greater importance as satellites are put into orbits which place them in the radiation belts. We had access to the linear accelerator at the Michael Reese Medical Center, \* and a series of experiments were performed that examined the kinetics of formation and bleaching of color centers in fused silica. This is by no means a complete experiment and a good deal of further work is indicated.

We choose to study fused silica, because of its obvious use as an optical window material (e. g. covering for solar cells). This material has been studied rather intensively, but even today the details of the defects are not completely known. The absorption bands due to the color centers have been studied by various workers. Mitchell and Paige<sup>(4)</sup> carefully studied quartz and fused silica, and have classified and labeled the various bands. The absorption band at 2200 Å (5.8 eV) is known as the C band. This band centers at 2150 Å in crystalline quartz, and shifts to 2200 Å in the fused silica. The bonding in quartz is somewhat uncertain but is a covalent with a partial ionic character.<sup>(5)</sup> Fused silica is not a completely amorphous material, but has a typical glassy structure with short range ordering. The silicon atom is bonded to four nearest oxygen atoms. It was generally accepted that a displaced oxygen atom was necessary to create the center which was thought to consist of an electron trapped at an oxygen vacancy,

---

\* We would like to thank Dr. J. O'Vadia, Chief Physicist in charge of the Accelerator, for his assistance in setting up the experiments.

but more recent evidence<sup>(6)</sup> indicates that the center consists of an ionized, strained Si-O bond. This hypothesis also helps to explain the greater colorability of fused silica which has of course a greater number of strained and broken bonds. It is also known that the C band can be bleached by ultraviolet light in the band 2000 - 3000 Å.

High purity fused silica shows only two major absorption bands. The C band at 2200 Å and the E band at 1870 Å in the vacuum ultraviolet. Small concentrations of impurities will show up as additional absorption bands notably at 5500 Å (2.26 eV) and 3000 Å (4.15 eV). These and others were present in our samples. It was not our purpose to study the detailed internal mechanisms of the formation of defects, but rather to study the kinetics of formation and bleaching of the color centers. We are particularly interested in the combined effects of the high energy particles, and the ultraviolet radiation. Three phases were envisioned:

1. Coloring rate dependence on radiation dose
2. Bleaching rate dependence on ultraviolet dose
3. Coloring and bleaching rates when particles and ultraviolet radiation are present together.

Part one was not carried out by us, but has been reported in the literature. We did carry out the other two parts, although because of the vastly different coloring and bleaching rates Part 3 was of doubtful value, and indeed no effects were seen. The high intensity of the electron beam ( $10^6$  rad/min) requires a high intensity ultraviolet source to cause observable effects. This indicates one of the problems of these experiments: compatibility between the various radiation sources. We have used three different sources, a small mercury lamp, a hydrogen arc lamp and a 1 KW xenon lamp.



This small lamp put about  $0.1 \mu\text{W}/\text{cm}^2$  of the 2537 line of mercury on the sample. We later tried bleaching with this lamp and the hydrogen arc, but neither source gave noticable bleaching in any reasonable time period. We did our later bleaching experiments with a 1 KW xenon arc lamp whose power and spectral output are not known accurately, but typically xenon lamps of this type have a continuum output in the region 2000 - 3000 Å that has the same spectral characteristic as a  $6000^\circ\text{K}$  black body. The actual power level is not known, but could be measured with a calibrated thermopile.

The bleaching was done by cementing the colored sample to an aperture disk and measuring the absorption as a function of wavelength. The aperture was then placed in the ultraviolet source and bleached for say 10 minutes. Another absorption measurement was then made. This procedure was repeated. Several runs were made out to 1 hour. To see the long term trends a sample was bleached for 17 hours. This removed almost all of the coloring and is perhaps not a good data point. The bleaching of the two major bands is shown in Figure III-1.

#### Experimental Results

A stack of 10 silica slabs 10 x 20 x 1 mm with aluminum foil interleaved to mask one-half of the length of the slab was placed in the beam. The silica was simultaneously irradiated by ultraviolet from the side. The slab was irradiated for 3 minutes. Tests were also made with small round samples aluminized over 1/2 of the surface. These gave essentially the same results.

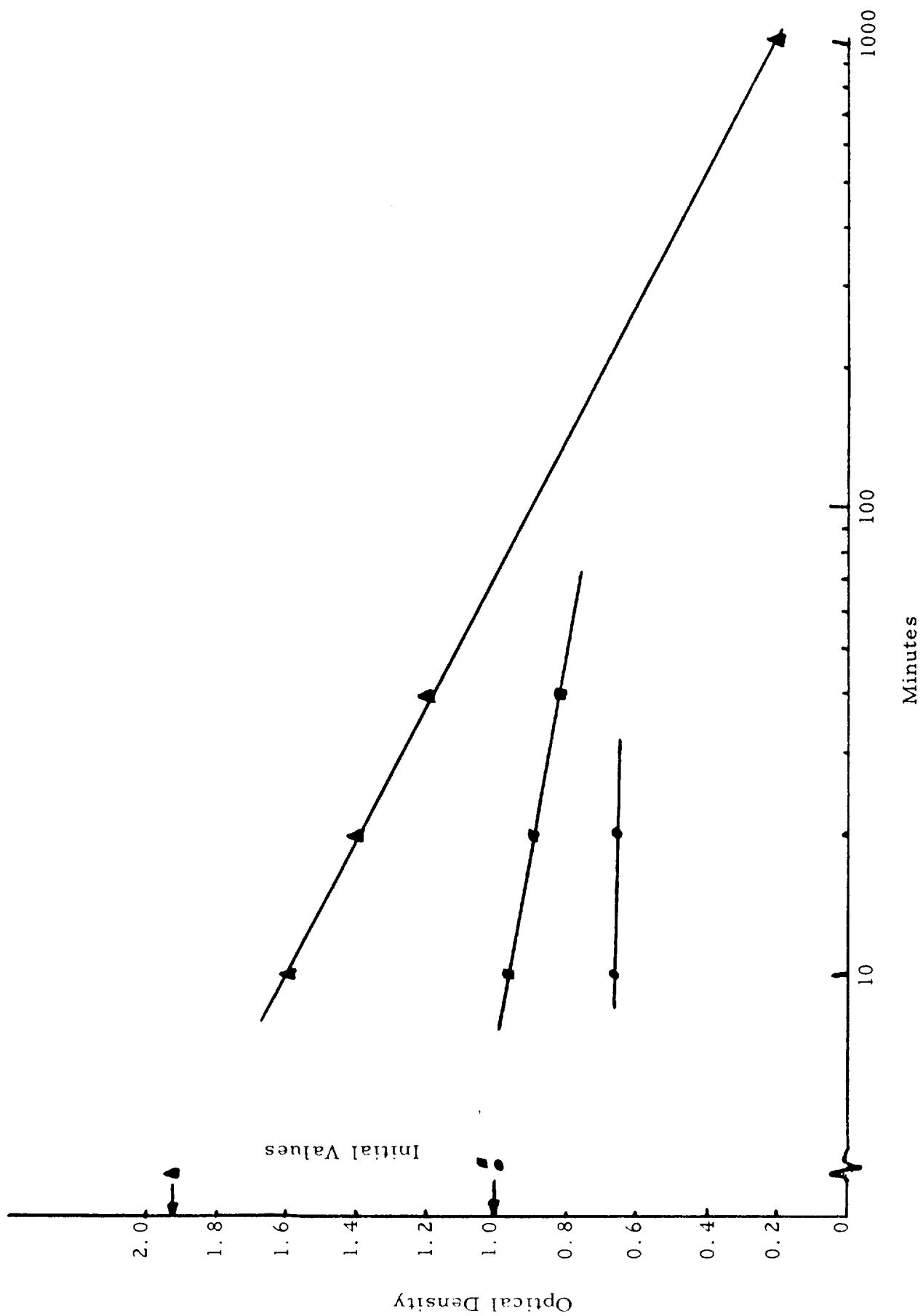


Figure III-1 Bleaching of Color Centers in Fused Silica.

After even short exposures the samples are rather evenly colored purple. This is due to the impurity band at 5500 A. The more interesting band at 2200 A cannot be observed visually, but photometer measurements show that this absorption is also rather uniform throughout the sample. This is contrary to our previous experience with glass. Normally the main electron beam leaves an intense track, with a peripheral region of light coloring due to scattered particles riding along with the main beam. The ordinary glasses are similar to fused quartz in that their main constituent is silica, but they contain, in addition, other oxides often of the heavier elements. We do not have an explanation for this phenomena. One additional interesting point is that the 5500 A coloring was concentrated along the striations in the silica. This absorption band is due to an aluminum impurity, and it is likely that these impurities gather along the striations. There is no reason to assume that the quartz-structure absorption bands are more intense along the striations unless there was evidence that there were more strained or broken bands along the striations.

We were unable to detect any difference in density between electron irradiation only, and electron irradiation in the presence of the ultraviolet radiation. Because of the limited output of the lamp used we cannot preclude any lack of effect. There are several important loss mechanisms for high energy electrons, including collision, ionization and excitation, and radiation. The following expression, first given by Bethe, may be found in most standard texts on elementary nuclear physics. It gives the loss due to collision and ionization, which are not essentially different processes, when the energy

of the incident particle is relativistic

$$-\left(\frac{dT}{dx}\right) = \frac{2\pi e^4 Z N}{mV^2} \frac{\ln m V^2 T}{2 I^2 (1 - \beta^2)} - \ln 2 (2\sqrt{1 - \beta^2} - 1 + \beta^2) \\ + (1 - \beta^2) + \frac{1}{8} (1 - \sqrt{1 - \beta^2})^2$$

where  $Z$  is nuclear charge,  $N$  is density of atoms in material,  $T$  is the relativistic energy, and  $I$  is the average excitation potential.

The average excitation potential may be computed by weighing the potential for each electron shell by the number of electrons in the shell. Average ionization potentials may be measured, calculated or interpolated from known materials. F. W. Spiers<sup>(7)</sup> has given values for some of the common materials; these are listed in Table III-1. One may calculate the energy loss using Bethe's expression. However, for very energetic particles there are losses due to radiation (bremstrahlung), and for polarizable media there is an additional correction necessary. This is discussed by Johns and Laughlin<sup>(8)</sup> who give values for water listed in Table III-2.

A commonly used unit of radiation is the rad which corresponds to the deposition of 100 ergs/gram of material. The Michael Reese Linac has a beam energy deposition rate of  $10^6$  rad/min over 1 mm diameter of the beam. This of course refers to tissue or water and must be re-evaluated for other materials such as quartz. The energy loss depends on the density of atoms and the effective charge per atom. We can see that it is then effectively dependent on the mass density of the material. So for thin sections, where the energy deposition is uniform, fused silica (density 2.2) will receive

TABLE III-1  
AVERAGE EXCITATION POTENTIALS

Material	I (ev) Experimental Values
hydrogen	15.6
lithium	34.0
beryllium	60.4
carbon	76.4
aluminum	150
iron	241
copper	276
silver	418
tin	463
tungsten	655
lead	705
uranium	811
air	80.5
Material	Interpolated Values
helium	26.9
nitrogen	87.7
argon	192
oxygen	98
	Calculated Values
water	68.0
anthrocene	64.6
polyethylene	51.4
polystyrene	60.5
lucite	65.4
bakelite	68.8

TABLE III-2  
ENERGY LOSS BY ELECTRONS IN WATER

<u>Energy Mev</u>	<u>Collision</u>	<u>Polarization Correction</u>	<u>Radiation</u>
0.01	23.0	----	----
0.1	4.19	----	----
1.0	1.885	- 0.026	0.006
2.0	1.91	- 0.069	0.023
5.0	2.07	- 0.144	0.078
10.0	2.25	- 0.243	0.196
20.0	2.41	- 0.350	0.475
50.0	2.64	- 0.499	1.390
100.0	2.80	- 0.606	2.814

(All energy losses given as MEV/cm)

a dose of  $2 \times 10^6$  Rad. The electrons will lose about 6.75 mev/cm, so for thin sections the total energy loss will be negligible. Without more accurate dose rate measurements we are forced to assume the validity of these numbers. Dr. O'Vadia of the Michael Reese staff has made measurements which yield isodose curves for the beam, and in general one knows quite well the dose rate as a function of position in the beam. We would have made more extensive use of this data, but for the anomalous coloring which did not seem to depend on the dose rate except in some gross way, it would appear that the bulk of the coloring was due to x-rays emitted when the electrons interact with the quartz. Previous work with glass has given coloring that was extremely dose dependent, and glass plates show coloring duplicating that in the film emulsions used in dose measurements.

#### IV. SPUTTERING BY HIGH ENERGY ARGON IONS

During the course of this program we engaged Dr. R. Hines of Northwestern University as a Consultant. Dr. Hines was engaged in the measurement of the sputtering yield of quartz and glass, and has published his results in the field.<sup>(9)</sup> Dr. Hines' facility could be used to sputter materials under high vacuum conditions ( $10^{-5}$  -  $10^{-6}$  torr) with the rare gases, say argon, at energies up to 40 kV. A small ion beam is swept over an area of approximately 1 sq. mm. This has the advantage of high current density, which is important if the residual gas pressure is relatively high, and also gives a reasonable area for measurements. Provision is incorporated into the facility for a source of neutralizing electrons. This is required with insulators. Dr. Hines bombarded series of materials as shown in Table IV-1. To insure uniform current density a small diameter beam was swept to provide a total area of  $0.04 \text{ cm}^2$ . The insulators were neutralized by electrons from an auxillary filament. The bombardments were carried out in only a moderately good vacuum so that thin polymerized oil films formed on the surface.

TABLE IV-1  
LIST OF SPUTTERED MATERIAL

<u>Material</u>	<u>Ion</u>	<u>Energy (kev)</u>	<u>Ion Current (<math>\mu</math>amps)</u>	<u>Time Sec</u>
Glass	A <sup>+</sup>	40	5.1	1200
Aluminized mylar	A <sup>+</sup>	40	4.6	1200
KCL	A <sup>+</sup>	40	5.6	900
NACL	A <sup>+</sup>	40	5.2	1200
Germanium	A <sup>+</sup>	40	4.3	1200
Sapphire	A <sup>+</sup>	40	4.6	1200

Only preliminary results were obtained. We originally planned to make additional, more quantitative, measurements, but Professor Hines was unable to continue as a consultant. All the samples were examined with an optical microscope and in addition optical absorption measurements were made with a Cary spectrophotometer. For most of the materials very little damage was apparent. The aluminized Mylar unfortunately melted. If the temperature were controlled one would expect to see erosion of the thin aluminum film, with perhaps some damage to the Mylar backing. The aluminum thickness was chosen to be one-half the range of 40 Kev argon ions. This should lead to some interesting effects, but the experiment would have to be redone with a lower-power density in the beam. Because of the applications of metallized Mylar surfaces (e. g. or reflectors or antennas) this would be an interesting point to pursue, and is related to the other experiments on thin films at low energy.

The range of these ions in most materials is very limited and any radiation damage effects while quite intense will be limited to a very thin layer on the surface. As a consequence bulk effects such as optical absorption are limited. Surface effects such as photoemission, photoconductivity, and change in reflectivity may be more prominent, but could not be measured due to the limitation in time.

Attempts at a measurement of optical absorption was generally unsuccessful. A change in the reflectance of quartz has been previously measured by Hines, but as noted above this is expected to have little effect on the bulk properties. The microscope studies showed some damage apparent on the KCl, NaCl and germanium. The sapphire showed no evidence of sputtering, but because of the rough surface one cannot say that there was



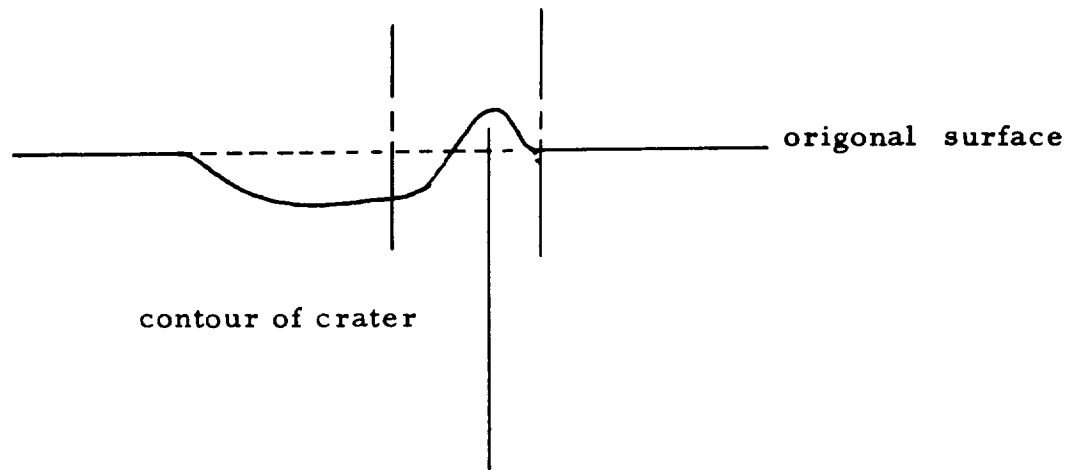
no sputtering. The salt crystals appeared to have suffered some surface erosion and also a change in the surface characteristic (i. e. certain markings on the surface were obliterated). The germanium single crystal showed the most damage. This slice of germanium had been polished so that surface changes were easily seen. There was a discoloration of the surface due to the oil film, but there was an additional change in reflectance possible due to surface changes. There was an obvious crater with a strange effect around the rim. See Figure IV-1. Microphotographs and electron micrographs (figures IV-2, IV-3 and IV-4) were also taken of the area near the edge of the crater. These showed an agglomeration of pits. The bottom of the crater was smooth. However, various scratch marks were still present, and may have been made after bombardment.

The contour at the edge of the crater was determined by means of fringe shift using an interferometer head for the microscope. This head was also used to determine film thicknesses for the sputtering experiments. No attempt was made to measure sputtering ratios although this could be done by measuring either weight loss for small samples or by measuring the volume of the crater by use of interference rings as suggested by Hines.<sup>(9)</sup> The sputtering ratios of the oxides and other compounds are not well known and very little quantitative work has been done.

It is generally believed that sputtering ratios for oxides and similar materials are low although a few measurements have been made. It is probable that these low values are due to the bond mechanisms and crystal structure. It would be desirable to study the sputtering of these materials especially in the low energy region. This would add to the knowledge of basic sputtering phenomena. If the theory of sputtering can be refined it could also aid the general understanding of the chemical bond, surface bond energies, displacement energies and other related phenomena in solids.

## REFERENCES

1. Daniel McKeown, Rev. Sci. Inst. 32, 133 (1961).
2. Gunter Sauerbrey, Zeit. fur Physik 155, 206 (1959).
3. Nils Lagried and G. K. Wehmer, Jour. Appl. Phys. 32, 365 (1961).
4. E. W. J. Mitchel and F. G. S. Paige, Phil. Mag. 1, 1055 (1956);  
Phil. Mag. 46, 1353 (1955).
5. Pauling, L. The Nature of the Chemical Bond, 3rd Ed. Chapter 3,  
Cornell Univ. Press, (1960).
6. W. Dale Compton and George W. Arnold, Jr., Discussions of the  
Faraday Soc. #31, p. 130 (1962).
7. F. W. Speirs, Radiation Dosimetry, p. 29, G. S. Hines and  
G. L. Brownell, ed's., Academic Press 1956.
8. H. E. Johns and J. S. Laughlin, Radiation Dosimetry, p. 100, Hines  
and Brownell, ed's., Academic Press 1956.
9. R. Hines and R. Wallor, Jour. Appl. Phys. 32, 202 (1961).



interferometer fringe showing shape of crater

Figure IV-1 SHAPE OF CRATER IN SPUTTERED GERMANIUM



a) Magnification 246 X



b) Magnification 1280 X

Figure IV-2 Microphotograph of Sputtered Germanium.



Figure IV-3    Electron Micrographs of Edge of Crater Made  
With Palladium-Carbon Replicas.



**Figure IV-4      Electron Micrographs of Center of Crater Made  
With Palladium-Carbon Replicas.**

APPENDIX A

REQUIREMENTS OF AN ULTRA-HIGH VACUUM  
SPUTTERING FACILITY

The investigation of the system requirements and preliminary design of an ultra-high vacuum facility were completed under NASA Project NASr-29. The general principles, and a tentative design were presented in the first quarterly report, ARF 1188-1, after extensive discussion and investigation of existing systems. This Appendix gives a summary of the previous material.

Many of the earlier sputtering yield data were obtained under rather dubious conditions. As Yonts and Harrison<sup>1</sup> showed, rather gross effects can result from too high an ambient pressure. If one is to do an ion beam experiment kinetic high vacuum conditions must be maintained. If a discharge type is contemplated only static high vacuum conditions apply.

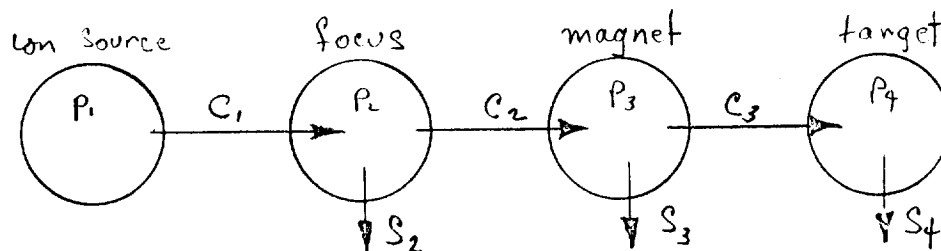
The basic requirement is an all metal bakeable system. The now standard techniques must be used (e. g. stainless steel--heliarc welded, with polished welds and a fine surface finish). Metal gaskets should be used, but since large bakeable valves are still difficult to obtain we will probably have to include some kind of a gasket, say viton or something similar which can be baked to about 300°C.

We propose a mass analyzed ion beam and hence require a high pumping speed. To keep pumping requirements at a minimum, the ion source should have a good gas efficiency and should give a high current density. A mass analyzer is most important for work with light ions. For example, 600 ev a mercury ion has a sputtering yield of approximately one,<sup>2</sup> but hydrogen for the same energy has a yield of about 0.01. Therefore each mercury ion will cause as much sputtering as 100 protons. Thus to get a one percent

accuracy in light ion yield determination, the heavy ion concentration must be less than one in  $10^4$ . The spread in the ratios increases with energy at 10 kev impurity levels must be less than 1 in  $10^5$ .

There is an inter-relation between current, current density, sputtering yield and pressure that allows us to determine the required pumping speed. The ambient gas molecules will impinge on the surface at a rate determined by gas pressure and temperature. Contamination layers will build up on a surface at a rate determined by this random gas current density and the sticking probability (the problem is particularly serious for such active species as oxygen much less so for the rare gases which do not tend to form multi layers). If we assume a ion beam density of  $100 \mu\text{a}/\text{cm}^2$ , which should be attainable and also gives a reasonable power input of  $1 \text{ W}/\text{cm}^2$  at 10 kv, then a pressure of  $10^{-8}$  torr is required to give an ion-to-molecule ratio of 100. This ratio may be marginal if long running times are required.

We may now estimate the pump requirements by choosing a total current of say  $100 \mu\text{a}$  (which corresponds roughly to  $6 \times 10^{12}$  ions/sec). If we want a pressure in the test chamber of say  $10^{-9}$  torr we will require a pumping speed of  $152 \text{ l}/\text{sec}$  for just the ions. The ionization efficiency of the ion source is about 10 percent, so we must only extract the ions and inhibit the gas flow, also we must hold the pressure down in the region where the ion beam travels to prevent scattering. These and other considerations lead one to consider a differentially pumped system, as shown schematically below.





We have four regions connected by apertures, or tubes, of conductance C to limit the gas flow but not the ions. Three of the regions are pumped at speed S. We tabulate the results of the calculations below

Region	C	S	P
1	$10^{-2}$ l/s		$10^{-3}$ torr (assumed)
2	.30 l/s	8 l/s 4" diffusion pump	$10^{-6}$ torr
3	.35 l/s	50 l/s 6" diffusion pump	$10^{-7}$ torr
4	-----	500 l/s 10" diffusion pump	$.7 \times 10^{-10}$ torr    static  $10^{-9}$ torr with ion beam on

The calculations assume no scattering out of the ion beam, but include some allowance for wall out-gasing and for the additional material introduced by high sputtering yields. The pumping speeds are for trapped and baffled pumps.

We have also considered magnetic deflection systems for mass (or energy) analysis. There are techniques to get second order focusing and perhaps to get a spot focus. There is some judgement to be exercised in choice of the deflection angle as it effects the focal length and the total path length required which will in turn effect the spread of the beam due to space charge effects. These factors must be weighed against magnet volume required to give the most economical design possible. We have completed a preliminary design for such a vacuum system. This was done after consultation with various manufacturers and designers of high vacuum equipment. The system would be all stainless steel and would use  $90^{\circ}$  beam deflection which best suits the dual requirements of space and focus.

Mercury diffusion pumps would be used, as they have been shown to be superior to oil in that the Hg can be more efficiently trapped out of the system. Oil pumps must be double trapped to prevent oil migration.

#### REFERENCES

1. O. C. Yonts and D. E. Harrison, J. Appl. Phys. 31, 1583 (1960).
2. G. Wehner, General Mills Report 2309.

APPENDIX B  
STATIC ULTRA HIGH VACUUM SYSTEM

In the study of thin film sputtering a simple glass vacuum system was used. This system had ground glass greased joints, and was pumped by a Vac-Ion pump to a pressure of  $10^{-8}$  torr between runs. The system may be seen in Figures B-1 to B-3. A combination of direct heating and gas discharge cleaning was used to clean up the system before use. Not shown in the pictures is the gas handling system for high purity gases in glass flasks, which was used when the tank grade proved inadequate.

The system consists of a tube which passes through a solenoid; at one end of this tube is mounted the crystal detector and a system of shields. At the other end is a tungsten filament, and accelerating electrodes. The system was supposed to operate at a pressure of  $10^{-4}$ - $10^{-5}$  torr, and a low intensity beam of ions was to be accelerated to the target. In practice we generally ran the system at 50-100 microns in a discharge mode, and ions were extracted from the plasma. This is simple, but unfortunately the ions have a large energy spread, and to make such a system practical at low energies a retarding field technique should be used.

The quartz crystal scheme of McKeown was used to detect mass changes. An oscillator circuit was constructed as shown in Figure B-4. The temperature characteristics of the crystals were measured by cycling the crystal through the temperature range - 70 to + 70°C. It can be seen in Figure B-5 that the crystal is stable to within plus or minus one cycle in the temperature range + 10 to + 50°C.

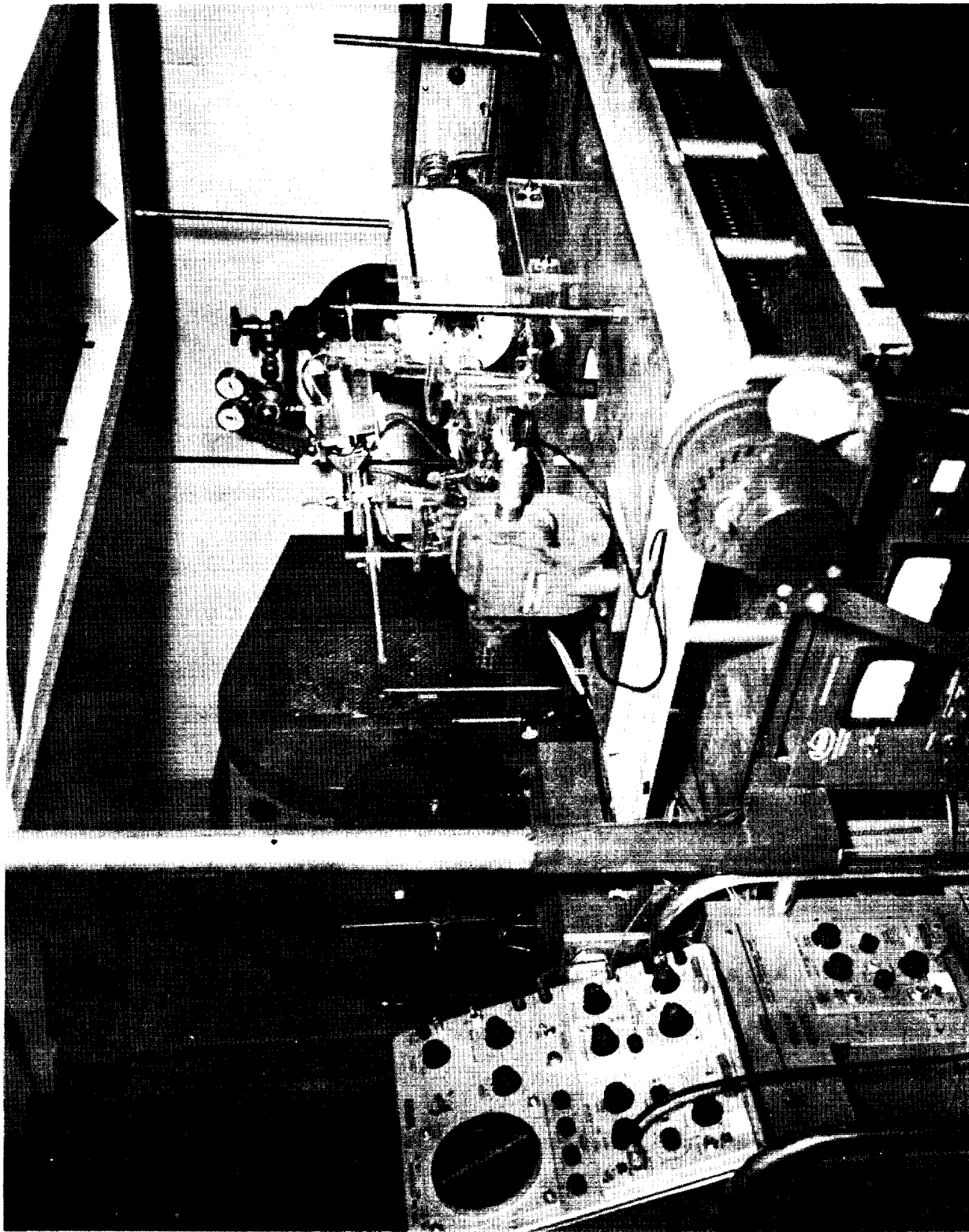


Figure B-1 Static Vacuum System.

45 ~~2~~

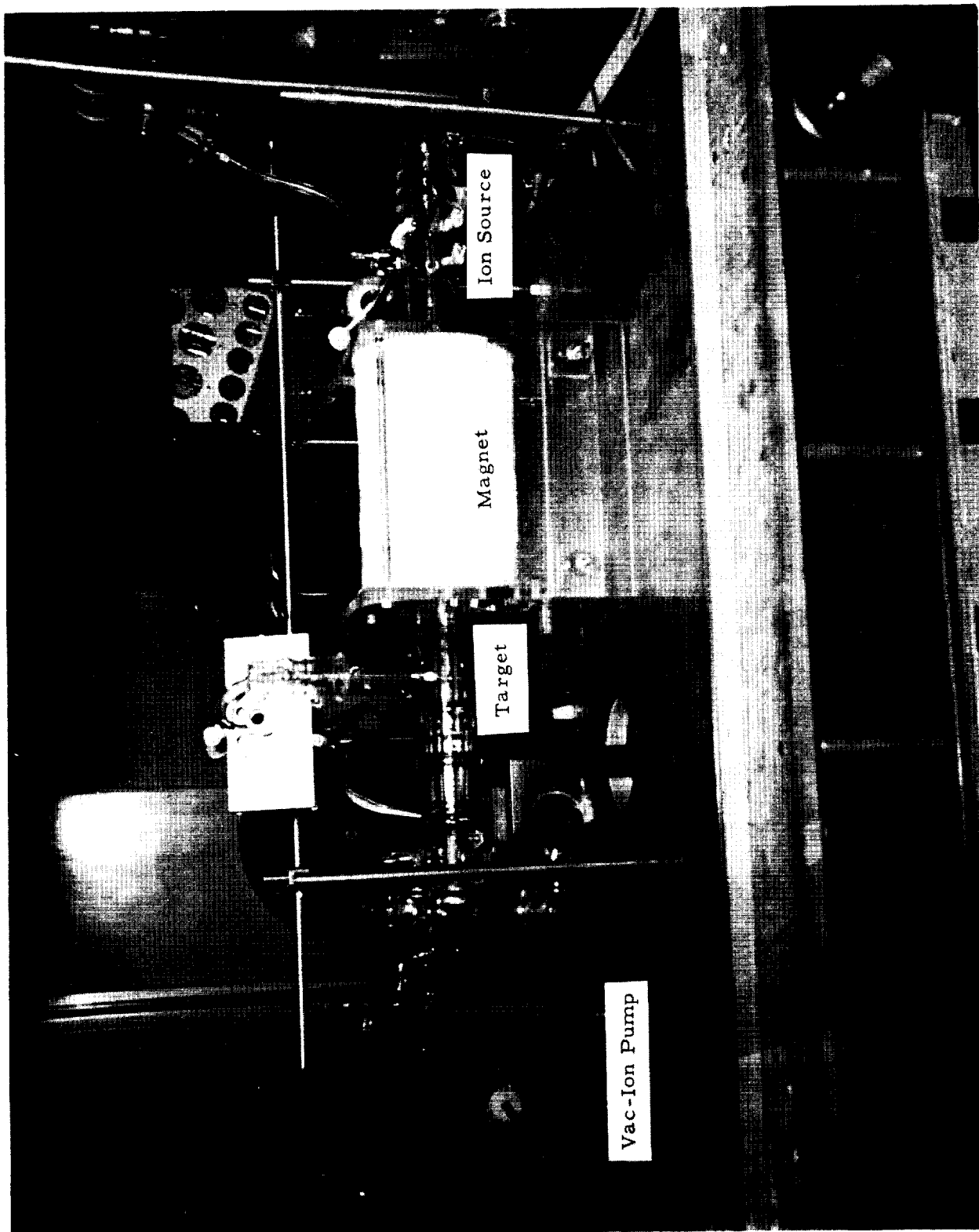


Figure B2. Closeup of Static Vacuum System

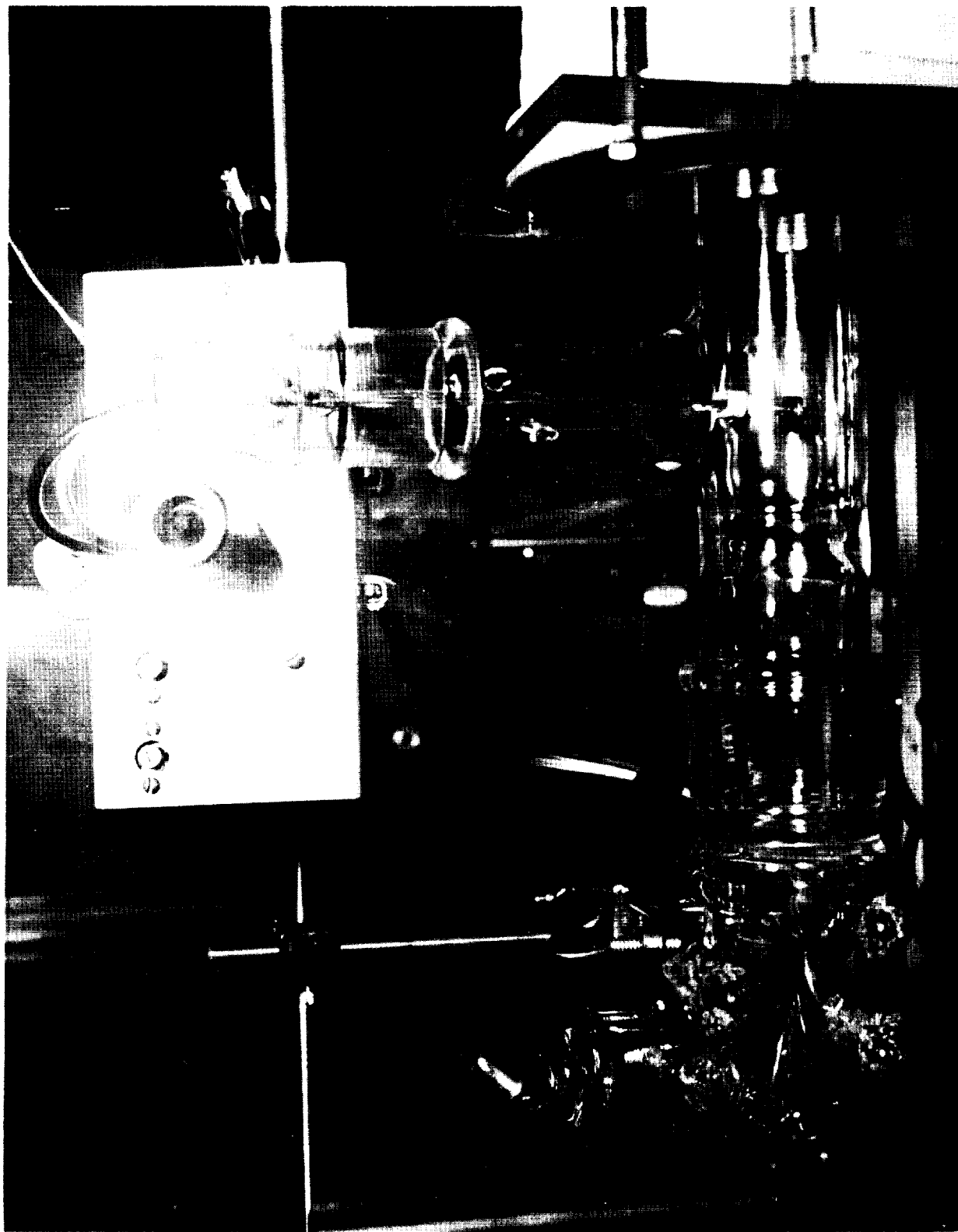


Figure B-3 Crystal Holder and Oscillator.

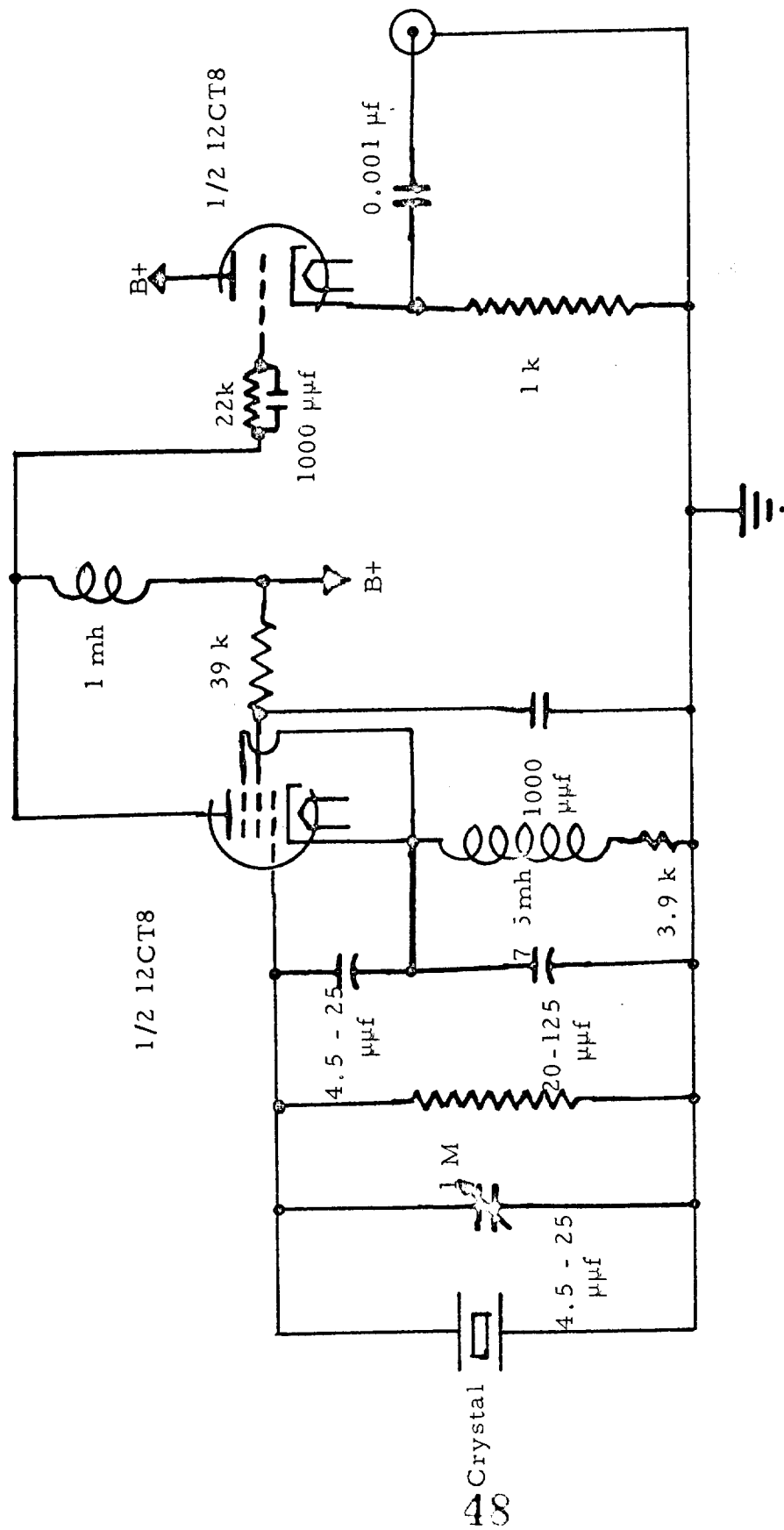


Figure B4. Crystal Oscillator Circuit

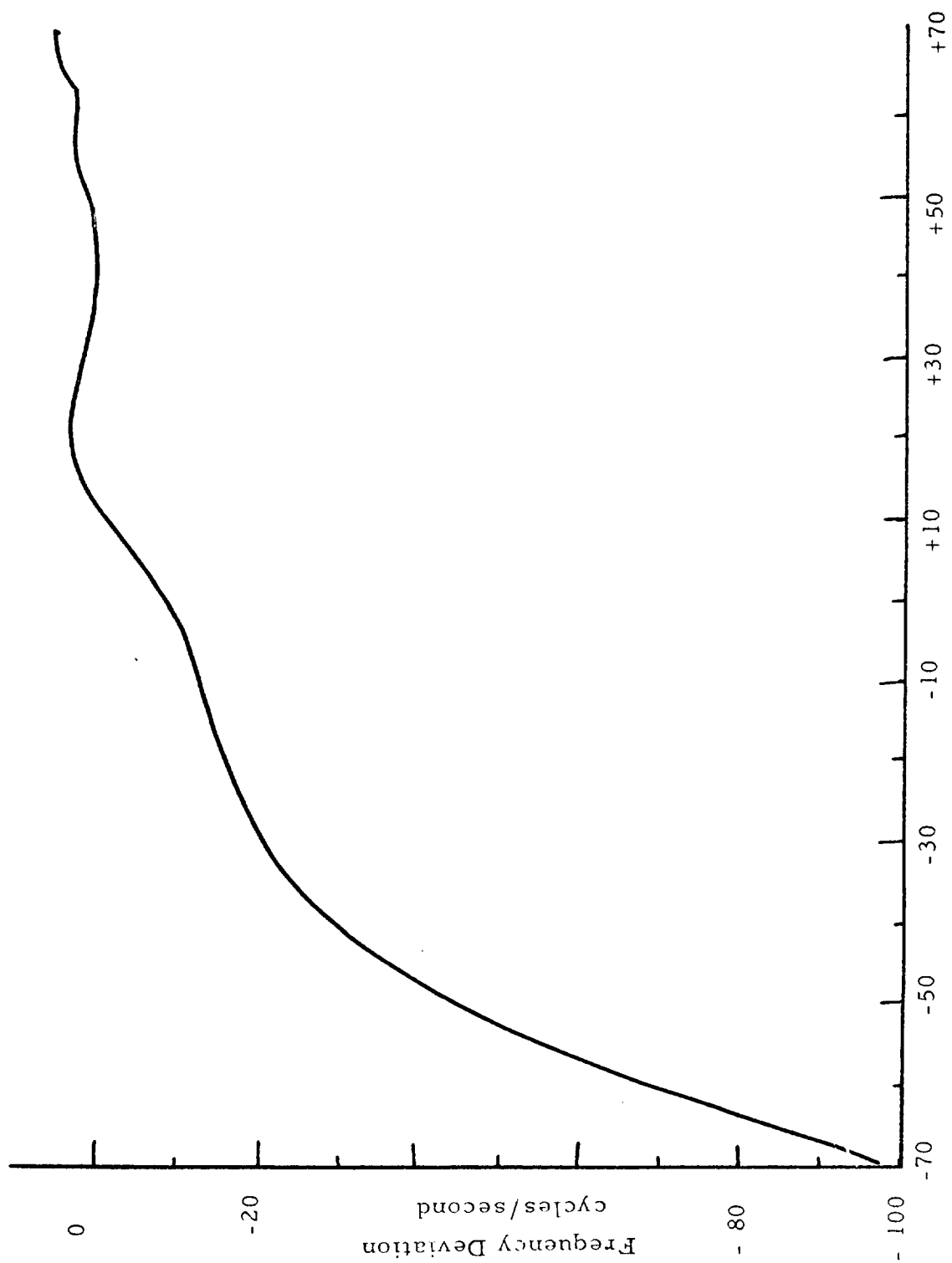


Figure B5. Temperature Dependence of Crystal Frequency



### DISTRIBUTION LIST

This report is being distributed as follows:

<u>No. of Copies</u>	<u>Recipient</u>
25	Office of Research Grants and Contracts Code BG National Aeronautics and Space Administration Washington 25, D. C.
4	Mr. Herbert W. Talkin NASA Headquarters Room H526, Code DA 1520 H Street, Northwest Washington 25, D. C.
4	Dr. R. Raring NASA Headquarters 1520 H Street, Northwest Washington 25, D. C.
4	Dr. Michael C. Bader Ames Research Center Moffet Field, California
1	Dr. J. O'Vadia Michael Reese Medical Center Chicago 16, Illinois
	<u>Armour Research Foundation</u>
1	R. G. Stewart
1	L. C. Scholz
1	Division A Files
1	Main Files
1	Report Library via Research Advisor
1	Plasma and Electron Physics Research File

